INTERNATIONAL JOURNAL FOR NUMERICAL METHODS IN FLUIDS
Int. J. Numer. Meth. Fluids 2013; **71**:1369–1381
Published online 14 August 2012 in Wiley Online Library (wileyonlinelibrary.com/journal/nmf). DOI: 10.1002/fld.3716

Adaptive variational multiscale method for the Stokes equations

Lina Song[1], Yanren Hou[1,2,*,†] and Haibiao Zheng[1]

[1]*School of Mathematics and Statistics, Xi'an Jiaotong University, Xi'an 710049, China*
[2]*Center for Computational Geosciences, Xi'an Jiaotong University, Xi'an 710049, China*

SUMMARY

An adaptive variational multiscale method for the Stokes equations is presented in this paper. We solve the coarse scale problem on the coarse mesh and approximate the fine scale solution by solving a series of local residual equations defined on some local fine grids, which can be implemented in parallel. In addition, we also propose a reliable local a posteriori error estimator and construct an adaptive algorithm based on the corresponding a posterior error estimate. Finally, numerical examples are presented to verify the algorithm. Copyright © 2012 John Wiley & Sons, Ltd.

Received 19 October 2011; Revised 17 June 2012; Accepted 30 June 2012

KEY WORDS: variational multiscale method; adaptivity; error estimator; the Stokes equations

1. INTRODUCTION

The incompressible Stokes equation is a basic and model problem in computational fluid dynamics. The a posteriori error estimation for finite element approximations to this problem has been studied by many researchers (see, e.g., [1–5]). Adaptive finite element methods based on rigorous a posteriori error estimators are efficient in the simulation of problems with various singularities.

The variational multiscale (VMS) method, proposed by Hughes and his co-authors [6, 7], has been widely used in computational fluid and solid mechanics. Its main idea is the scale decomposition, and its difficulty lies in computing a fine scale solution which has nonlocal effect on the coarse scale solution. To overcome such a difficulty, Layton [8], Kaya, and Riviere [9], and John and Kaya [10] construct an appropriate subspace depending on the coarse scale and on an additional viscosity stabilized parameter in order to model the effect between the fine and the coarse scales. Following this idea, Zheng and his co-authors [11–13] improve this method based on the Gauss integration. Alternatively, Larson and M*å*lqvist [14] localize the fine scale variational equation over patches of elements through a partition of the unity. Moreover, they derive an a posteriori error estimator in order to improve the reliability of the localization, and their method is also applied to mixed finite element methods [15].

The purpose of this paper is to develop an efficient a posteriori error estimator based on the local fine scale equations for the VMS finite element approximation to the Stokes equation. It is important to note that the fine scale solution may be regarded as not only a correction but also a residual of the coarse scale solution. Therefore, it is natural to use the energy norm of the fine scale approximation as an a posteriori error estimator for the coarse scale approximation. Obviously, there is no additional computation cost for such an estimator, and hence, the corresponding adaptive algorithm is efficient. It saves times and memories of the computer to solve a problem. In this paper, by the virtue of the a posteriori error estimation, we show theoretically and numerically that this estimator is dominante.

*Correspondence to: Yanren Hou, School of Mathematics and Statistics, Xi'an Jiaotong University, Xi'an 710049, PR China.
†E-mail: yrhou@mail.xjtu.edu.cn

This paper is organized as follows. Section 2 briefly introduces the Stokes equation, and Section 3 describes the VMS method and the error estimator based on the numerical realization of the method. Representative numerical examples are carried out in Section 4 to show the efficiency of the method. We will conclude our presentation in Section 5 with a few comments and possible future research topics as well.

2. MODEL PROBLEM

Consider the homogeneous Dirichlet boundary value problem for the Stokes equations

$$\begin{cases} -\nu\Delta \boldsymbol{u} + \nabla p = \boldsymbol{f} & \text{in} \quad \Omega, \\ \nabla \cdot \boldsymbol{u} = 0 & \text{in} \quad \Omega, \\ \boldsymbol{u} = 0 & \text{on} \quad \Gamma, \end{cases} \tag{1}$$

where $\Omega \subset R^d$, $d = 2\ or\ 3$, represents a polygonal domain with the Lipschitz continuous boundary $\Gamma = \partial\Omega$; $\boldsymbol{f}$ is a prescribed body force; $\boldsymbol{u}$ and p denote the velocity field and the pressure, respectively; and $\nu > 0$ is the kinematic viscosity.

First, we introduce some notations. Set $Y = \boldsymbol{X} \times M$, where $\boldsymbol{X} = H_0^1(\Omega)^d$ and M is a subspace of $L^2(\Omega)$ defined by

$$M = L_0^2(\Omega) = \left\{ q : q \in L^2(\Omega), \int_\Omega q dx = 0 \right\}.$$

The scalar product and the induced norm in M are denoted by the usual L^2 inner product and $\|\cdot\|_0$, whereas the scalar product and the induced norm in $\boldsymbol{X}$ are denoted by $((\boldsymbol{u}, \boldsymbol{v})) = (\nabla \boldsymbol{u}, \nabla \boldsymbol{v})$ and $\|\cdot\|_1$, respectively.

Then, the weak formulation for Equation (1) reads as follows: find $(\boldsymbol{u}, p) \in Y$ satisfying

$$B((\boldsymbol{u}, p); (\boldsymbol{v}, q)) = (\boldsymbol{f}, \boldsymbol{v}) \quad \forall (\boldsymbol{v}, q) \in Y, \tag{2}$$

with

$$a(\boldsymbol{u}, \boldsymbol{v}) = \nu((\boldsymbol{u}, \boldsymbol{v})),\ d(\boldsymbol{v}, q) = (\nabla \cdot \boldsymbol{v}, q),$$

$$B((\boldsymbol{u}, p); (\boldsymbol{v}, q)) = a(\boldsymbol{u}, \boldsymbol{v}) - d(\boldsymbol{v}, p) + d(\boldsymbol{u}, q).$$

It is well known that Y satisfies the following inf-sup condition for a certain constant β_0:

$$\inf_{q \in M} \sup_{\boldsymbol{v} \in \boldsymbol{X}} \frac{(q, \nabla \cdot \boldsymbol{v})}{\| q \|_0 \| \boldsymbol{v} \|_1} \geqslant \beta_0 > 0. \tag{3}$$

We now consider the finite element approximation to the Stokes equations in (1). Let τ_h be a regular triangulation of the domain Ω and define the mesh parameter

$$h = \max_{T \in \tau_h} \{diam(T)\}.$$

We choose the conforming velocity-pressure finite element space $Y_h = \boldsymbol{X}_h \times M_h \subset Y$ satisfying the discrete inf-sup condition

$$\inf_{q_h \in M_h} \sup_{\boldsymbol{v}_h \in \boldsymbol{X}_h} \frac{(q_h, \nabla \cdot \boldsymbol{v}_h)}{\| q_h \|_0 \| \boldsymbol{v}_h \|_1} \geqslant \beta > 0, \tag{4}$$

where β is a positive constant independent of h. Examples of such compatible spaces are the mini-element spaces [16], and the Taylor–Hood spaces [17].

Then, the Galerkin finite element discretization of (2) is given by the following: find $(\boldsymbol{u}_h, p_h) \in Y_h$ satisfying

$$B((\boldsymbol{u}_h, p_h); (\boldsymbol{v}_h, q_h)) = (\boldsymbol{f}, \boldsymbol{v}_h), \quad \forall (\boldsymbol{v}_h, q_h) \in Y_h. \tag{5}$$

DOI: 10.1002/fld

3. THE VARIATIONAL MULTISCALE METHOD

We use the VMS method proposed by Hughes [6, 7] to deal with the Stokes equations. We start by decomposing the solution space $Y = Y_c \oplus Y_f$, where Y_c is the coarse scale subspace and Y_f is the fine scale subspace. According to this space decomposition, the variational formulation Equation (2) yields the following coupled system of the following two subproblems: find $(\boldsymbol{u}_c, p_c) \in Y_c$ and $(\boldsymbol{u}_f, p_f) \in Y_f$ such that

$$\begin{cases} B((\boldsymbol{u}_c, p_c); (\boldsymbol{v}, q)) + B((\boldsymbol{u}_f, p_f); (\boldsymbol{v}, q)) = (\boldsymbol{f}, \boldsymbol{v}) & \forall (\boldsymbol{v}, q) \in Y_c, \\ B((\boldsymbol{u}_c, p_c); (\boldsymbol{v}, q)) + B((\boldsymbol{u}_f, p_f); (\boldsymbol{v}, q)) = (\boldsymbol{f}, \boldsymbol{v}) & \forall (\boldsymbol{v}, q) \in Y_f. \end{cases} \tag{6}$$

Now choose different compatible finite element spaces Y_H and Y_h to approximate the coarse scale space Y_c and the fine scale space Y_f, respectively. The corresponding mesh parameter h is much smaller than H. Then, the finite element approximation of Equation (6) reads as follows: find $\left(\boldsymbol{u}_c^H, p_c^H\right) \in Y_H$ and $\left(\boldsymbol{u}_f^h, p_f^h\right) \in Y_h$ such that

$$\begin{cases} B\left(\left(\boldsymbol{u}_c^H, p_c^H\right); (\boldsymbol{v}, q)\right) + B\left(\left(\boldsymbol{u}_f^h, p_f^h\right); (\boldsymbol{v}, q)\right) = (\boldsymbol{f}, \boldsymbol{v}) & \forall (\boldsymbol{v}, q) \in Y_H, \quad (a) \\ B\left(\left(\boldsymbol{u}_f^h, p_f^h\right); (\boldsymbol{v}, q)\right) + B\left(\left(\boldsymbol{u}_c^H, p_c^H\right); (\boldsymbol{v}, q)\right) = (\boldsymbol{f}, \boldsymbol{v}) & \forall (\boldsymbol{v}, q) \in Y_h. \quad (b) \end{cases} \tag{7}$$

It is clear that the much smaller size h leads to a quite larger linear system for the fine scale problem. To improve the computational efficiency of this large system, we approximate the fine scale problem Equation (7)(b) based on the localized Dirichlet problems.

3.1. Approximation of the fine scale problem based on localized Dirichlet problems

We use the method described by Larson [14] to decouple and localize the fine scale problem Equation (7)(b) for the Stokes equations.

We adopt the linear, Lagrange, basis functions $\{\phi_i\}_{i \in \mathcal{N}}$ on τ_H to be a partition of unity, where $\mathcal{N}$ is the set of coarse nodes on the mesh τ_H. For $i \in \mathcal{N}$, we denote by S_1^i the support of the basis function ϕ_i. Let $k \in \mathbb{N}$, define nodal patches of $k-$th order S_k^i by

$$S_k^i := \cup \left\{T \in \tau_H | T \cap \bar{S}_{k-1}^i \neq \emptyset\right\} \quad k = 2, 3, 4, \cdots .$$

Figure 1 shows the nodal patches of k-th order ($k = 1, 2, 3$). Each patch is uniformly refined with the mesh parameter $h = \frac{H}{4}$.

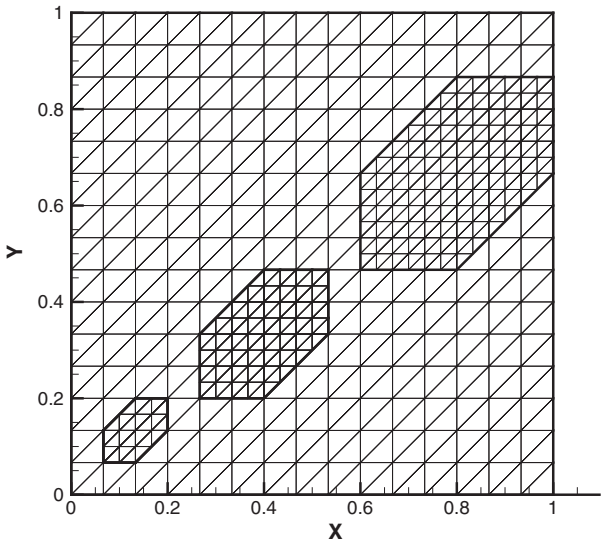

Figure 1. From left to right: nodal patches of k-th order ($k = 1, 2, 3$) with refinement.

DOI: 10.1002/fld

We choose S_k^i as the local domain ω_i about $i \in \mathcal{N}$. On each local domain ω_i, we define the fine scale solution space Y_h^i by $Y_h^i = \boldsymbol{X}_h^i \times M_h^i$, where

$$\boldsymbol{X}_h^i := \left\{ w \in \left[H_0^1(\omega_i) \right]^d \cap \boldsymbol{X}_h|_{\omega_i} \right\},$$

and

$$M_h^i := \left\{ q \in L_0^2(\omega_i) \cap M_h|_{\omega_i} \right\}.$$

Then, the approximation of the fine scale equation on each ω_i reads as follows: find $\left(\boldsymbol{u}_{f,i}^h, p_{f,i}^h \right) \in Y_h^i$ such that

$$B\left(\left(\boldsymbol{u}_{f,i}^h, p_{f,i}^h \right); (\boldsymbol{v}, q) \right) = (\boldsymbol{f}, \boldsymbol{v}\phi_i) - B\left(\left(\boldsymbol{u}_c^H, p_c^H \right); (\boldsymbol{v}\phi_i, q\phi_i) \right) \ \forall (\boldsymbol{v}, q) \in Y_h^i. \tag{8}$$

In conclusion, the VMS method for the Stokes equations reads as follows:
Find $\left(\boldsymbol{u}_c^H, p_c^H \right) \in Y_H$ and $\left(\boldsymbol{u}_{f,i}^h, p_{f,i}^h \right) \in Y_h^i$ such that

$$\begin{cases} B\left(\left(\boldsymbol{u}_c^H, p_c^H \right); (\boldsymbol{v}, q) \right) + B\left(\left(\hat{\boldsymbol{u}_f^h}, \hat{p_f^h} \right); (\boldsymbol{v}, q) \right) = (\boldsymbol{f}, \boldsymbol{v}) & \forall (\boldsymbol{v}, q) \in Y_H, \quad (a) \\ B\left(\left(\boldsymbol{u}_{f,i}^h, p_{f,i}^h \right); (\boldsymbol{v}, q) \right) = (\boldsymbol{f}, \boldsymbol{v}\phi_i) - B\left(\left(\boldsymbol{u}_c^H, p_c^H \right); (\boldsymbol{v}\phi_i, q\phi_i) \right) & \forall (\boldsymbol{v}, q) \in Y_h^i, \quad (b) \end{cases} \tag{9}$$

where $\left(\hat{\boldsymbol{u}_f^h}, \hat{p_f^h} \right) = \sum_{i \in \mathcal{N}} \left(\boldsymbol{u}_{f,i}^h, p_{f,i}^h \right)$. Then the final numerical solution is

$$(U, P) = \left(\boldsymbol{u}_c^H, p_c^H \right) + \left(\hat{\boldsymbol{u}_f^h}, \hat{p_f^h} \right).$$

3.2. The a posteriori error estimate based on the variational multiscale method

We define two special finite element spaces.

$Y_h^i(\omega_i)$: the restriction of the whole finite element space Y_h on the local domain ω_i. This space is identical to Y_h^i without the necessary zero boundary condition on $\partial\omega_i$.
$Y_h^i(\partial\omega_i)$: the restriction of $Y_h^i(\omega_i)$ on the boundary $\partial\omega_i$.

We use the graph norm $|||(\boldsymbol{v}, q)|||^2 = ||\boldsymbol{v}||_1^2 + ||q||_0^2 \ \forall (\boldsymbol{v}, q) \in Y$.

Theorem 3.1
Let $(\boldsymbol{u}, p) \in Y$ be the solution of the Stokes equations in (2) and $\left(\boldsymbol{u}_c^H, p_c^H \right)$ be the approximate solution of the Galerkin finite element method. Then, the error satisfies

$$||| \left(\boldsymbol{u} - \boldsymbol{u}_c^H, p - p_c^H \right) ||| \leqslant c \sum_{i \in \mathcal{N}} B_{f,i}^h + ||| \left(\hat{\boldsymbol{u}_f^h}, \hat{p_f^h} \right) |||. \tag{10}$$

Here, $B_{f,i}^h = \left(||\bar{\boldsymbol{u}}_{f,i}^h||_{\frac{1}{2},\partial\omega_i}^2 + ||\bar{p}_{f,i}^h||_{\frac{1}{2},\partial\omega_i}^2 \right)^{\frac{1}{2}}$, and $\left(\bar{\boldsymbol{u}}_{f,i}^h, \bar{p}_{f,i}^h \right) \in Y_h^i(\partial\omega_i)$ is the piecewise polynomial defined on $\partial\omega_i$ that uniquely solves

$$\left(\bar{\boldsymbol{u}}_{f,i}^h, \boldsymbol{v} \right)_{\partial\omega_i} + \left(\bar{p}_{f,i}^h, q \right)_{\partial\omega_i} = (\boldsymbol{f}, \boldsymbol{v}\phi_i) - B\left(\left(\boldsymbol{u}_c^H, p_c^H \right); (\boldsymbol{v}\phi_i, q\phi_i) \right) - B\left(\left(\boldsymbol{u}_{f,i}^h, p_{f,i}^h \right); (\boldsymbol{v}, q) \right), \tag{11}$$

for all $(\boldsymbol{v}, q) \in Y_h^i(\omega_i)$.

Proof
We can rewrite the Stokes equation (2) as follows.

$$B\left(\left(\boldsymbol{u} - \boldsymbol{u}_c^H, p - p_c^H \right); (\boldsymbol{v}, q) \right) + B\left(\left(\boldsymbol{u}_c^H, p_c^H \right); (\boldsymbol{v}, q) \right) = (\boldsymbol{f}, \boldsymbol{v}) \quad \forall (\boldsymbol{v}, q) \in Y. \tag{12}$$

DOI: 10.1002/fld

For any $(\boldsymbol{v}, q) \in Y_h \subset Y$, following Equation (11) and Equation (12), we obtain,

$$\begin{aligned}
&B\left(\left(\boldsymbol{u}-\boldsymbol{u}_c^H-\hat{\boldsymbol{u}_f^h}, p-p_c^H-\hat{p_f^h}\right);(\boldsymbol{v},q)\right)\\
&=(\boldsymbol{f},\boldsymbol{v})-B\left(\left(\boldsymbol{u}_c^H,p_c^H\right);(\boldsymbol{v},q)\right)-B\left(\left(\hat{\boldsymbol{u}_f^h},\hat{p_f^h}\right);(\boldsymbol{v},q)\right)\\
&=\sum_{i\in\mathcal{N}}(\boldsymbol{f},\boldsymbol{v}\phi_i)-B\left(\left(\boldsymbol{u}_c^H,p_c^H\right);(\boldsymbol{v}\phi_i,q\phi_i)\right)-B\left(\left(\boldsymbol{u}_{f,i}^h,p_{f,i}^h\right);(\boldsymbol{v},q)\right)\\
&=\sum_{i\in\mathcal{N}}\left(\bar{\boldsymbol{u}}_{f,i}^h,\boldsymbol{v}\right)_{\partial\omega_i}+\left(\bar{p}_{f,i}^h,q\right)_{\partial\omega_i}.
\end{aligned}$$

By the virtue of the inf-sup condition (4),

$$\begin{aligned}
&|||\left(\boldsymbol{u}-\boldsymbol{u}_c^H-\hat{\boldsymbol{u}_f^h},p-p_c^H-\hat{p_f^h}\right)|||\\
&\leqslant 2\beta^{-1}\sup_{(\boldsymbol{v},q)\in Y_h}\frac{B\left(\left(\boldsymbol{u}-\boldsymbol{u}_c^H-\hat{\boldsymbol{u}_f^h},p-p_c^H-\hat{p_f^h}\right);(\boldsymbol{v},q)\right)}{|||(\boldsymbol{v},q)|||}\\
&\leqslant 2\beta^{-1}\frac{|\sum_{i\in\mathcal{N}}\left(\bar{\boldsymbol{u}}_{f,i}^h,\boldsymbol{v}\right)_{\partial\omega_i}+\left(\bar{p}_{f,i}^h,q\right)_{\partial\omega_i}|}{|||(\boldsymbol{v},q)|||}.
\end{aligned}\tag{13}$$

The use of the trace inequality gives

$$\begin{aligned}
&|\sum_{i\in\mathcal{N}}\left(\bar{\boldsymbol{u}}_{f,i}^h,\boldsymbol{v}\right)_{\partial\omega_i}+\left(\bar{p}_{f,i}^h,q\right)_{\partial\omega_i}|\\
&\leqslant\sum_{i\in\mathcal{N}}\left(||\bar{\boldsymbol{u}}_{f,i}^h||_{\frac{1}{2},\partial\omega_i}||\boldsymbol{v}||_{\frac{1}{2},\partial\omega_i}+||\bar{p}_{f,i}^h||_{\frac{1}{2},\partial\omega_i}||q||_{-\frac{1}{2},\partial\omega_i}\right)\\
&\leqslant c\sum_{i\in\mathcal{N}}\left(||\bar{\boldsymbol{u}}_{f,i}^h||_{\frac{1}{2},\partial\omega_i}||\boldsymbol{v}||_{1,\omega_i}+||\bar{p}_{f,i}^h||_{\frac{1}{2},\partial\omega_i}||q||_{0,\omega_i}\right)\\
&\leqslant c\sum_{i\in\mathcal{N}}\left(||\bar{\boldsymbol{u}}_{f,i}^h||_{\frac{1}{2},\partial\omega_i}+||\bar{p}_{f,i}^h||_{\frac{1}{2},\partial\omega_i}\right)(||\boldsymbol{v}||_1+||q||_0).
\end{aligned}\tag{14}$$

Using Equation (13), Equation (14) and triangle inequality yields

$$\begin{aligned}
|||\left(\boldsymbol{u}-\boldsymbol{u}_c^H,p-p_c^H\right)||| &\leqslant |||\left(\boldsymbol{u}-\boldsymbol{u}_c^H-\hat{\boldsymbol{u}_f^h},p-p_c^H-\hat{p_f^h}\right)||| + |||\left(\hat{\boldsymbol{u}_f^h},\hat{p_f^h}\right)|||\\
&\leqslant c\sum_{i\in\mathcal{N}}B_{f,i}^h+|||\left(\hat{\boldsymbol{u}_f^h},\hat{p_f^h}\right)|||.
\end{aligned}$$

Here, $B_{f,i}^h=\left(||\bar{\boldsymbol{u}}_{f,i}^h||_{\frac{1}{2},\partial\omega_i}^2+||\bar{p}_{f,i}^h||_{\frac{1}{2},\partial\omega_i}^2\right)^{\frac{1}{2}}$. □

Remark

Note that the right hand of Equation (11) is equals to zero, for all $(\boldsymbol{v},q)\in Y_h^i$. That is because the local homogenous Dirichlet subproblem Equation (8) holds. Hence, in terms of calculation, Equation (11) is a linear system with a mass matrix defined on the boundary of the local domain ω_i.

It is the fact that $\left(\bar{\boldsymbol{u}}_{f,i}^h,\bar{p}_{f,i}^h\right)$ is closely related to the normal derivative of the fine scale solution $\left(\boldsymbol{u}_{f,i}^h,p_{f,i}^h\right)$ on the boundary of the local domain ω_i. The quantity $\left(\bar{\boldsymbol{u}}_{f,i}^h,\bar{p}_{f,i}^h\right)$ could be interpreted

DOI: 10.1002/fld

as a variational approximation of $n \cdot \left(\nu \nabla \boldsymbol{u}^h_{f,i} + I p^h_{f,i}\right)$, see [18]. $B^h_{f,i}$ will decrease as the size of the local domain increases. Because of such property, we could use this parameter to decide the size of the local domain.

Once the size of the local domain is decided, we use the energy norm of the fine scale approximation as the local error estimator η_T. More precisely, we define the error estimator as follows

$$\eta_T := |||\left(\hat{\boldsymbol{u}^h_f}, \hat{p^h_f}\right)|||_T = \left(||\sum_{i\in\mathcal{N}} \boldsymbol{u}^h_{f,i}||^2_{1,T} + ||\sum_{i\in\mathcal{N}} p^h_{f,i}||^2_{0,T}\right)^{\frac{1}{2}},$$

where $\left(\boldsymbol{u}^h_{f,i}, p^h_{f,i}\right)$ is the solution of Equation (9)(b) and the subscript T of the norm means the integration over the element T on the coarse mesh τ_H.

Moreover, we can define the global error estimator $\eta = \left\{\sum_{T\in\tau_H} \eta^2_T\right\}^{\frac{1}{2}}$.

4. NUMERICAL RESULTS

In this section, three experiments are presented to verify the efficiency and the reliability of the adaptive VMS method.

The algorithm in all experiments is implemented by the public finite element software Freefem++ [19]. Now, we state the adaptive algorithm for the VMS method.

- Step 1. Given the mesh τ^j_H, calculate a solution $\left(\boldsymbol{u}^j_H, p^j_H\right)$ by solving the problem Equation (5) with the standard Galerkin finite element method.
- Step 2. Replace $\left(\boldsymbol{u}^{H,j}_c, p^{H,j}_c\right)$ in the right hand of Equation (9)(b) with $\left(\boldsymbol{u}^j_H, p^j_H\right)$ and calculate a series of solutions $\left(\boldsymbol{u}^{h,j}_{f,i}, p^{h,j}_{f,i}\right)$ $(i \in \mathcal{N})$ by solving the local residual linear equations Equation (9)(b).
- Step 3. Calculate $B^{h,j}_{f,i}$ for each $i \in \mathcal{N}$. For the large value in $\left\{B^{h,j}_{f,i}\right\}_{i\in\mathcal{N}}$, increase the size of the corresponding local domain ω_i, and resolve the corresponding problem Equation (9)(b) on the extended domain.
- Step 4. Calculate $\left(\boldsymbol{u}^{H,j}_c, p^{H,j}_c\right)$ by solving the problem Equation (9)(a) with $\left(\hat{\boldsymbol{u}^{h,j}_f}, \hat{p^{h,j}_f}\right) = \sum_{i\in\mathcal{N}} \left(\boldsymbol{u}^{h,j}_{f,i}, p^{h,j}_{f,i}\right)$ and update the solution $(U^j, P^j) = \left(\boldsymbol{u}^{H,j}_c, p^{H,j}_c\right) + \left(\hat{\boldsymbol{u}^{h,j}_f}, \hat{p^{h,j}_f}\right)$.
- Step 5. Calculate the error estimator $\eta^j = \left\{\sum_{T\in\tau^j_H} ||\hat{\boldsymbol{u}^{h,j}_f}||^2_{1,T} + ||\hat{p^{h,j}_f}||^2_{0,T}\right\}^{\frac{1}{2}}$. Go to Step 6 or stop if η^j reaches the desired tolerance η^s.
- Step 6. Generate a new mesh τ^{j+1}_H by the refinement strategy in [19] based on the error estimator η^j. Go back to Step 1.

4.1. A singular problem

The example is a singular problem in a circular segment with the radius 1 and the angle 2π. We consider Ω as a disk of the radius 1 with a crack joining the center to the boundary as presented in [1, 12]. The exact velocity $\boldsymbol{u} = (\boldsymbol{u}_1, \boldsymbol{u}_2)$ and the pressure p are given as follows:

$$\boldsymbol{u}_1 = 1.5r^{1/2}(cos(0.5\theta) - cos(1.5\theta)),$$

$$\boldsymbol{u}_2 = 1.5r^{1/2}(3sin(0.5\theta) - sin(1.5\theta)),$$

$$p = -6r^{-1/2}cos(0.5\theta),$$

DOI: 10.1002/fld

where (r, θ) is a polar representation of a point in the disk. It is clear that the pressure p is singular at the end of the crack, that is, at the center of the disk. Hence, we expect that the refined meshes appear here.

The adaptive mesh refinement starts with the initial mesh τ_h^0 as shown in the left part of Figure 2. The algorithm provides a series of adaptive meshes $\left\{\tau_h^j\right\}_{j=1,2,3}$ in Figures 2 and 3. It shows that the adaptive algorithm introduces mesh refinements along the end of the crack, where the pressure is singular. On the other hand, the algorithm decides to increase the size of the local domain ω_i in the nodes marked with red dots in all mesh figures. This indicates that the normal derivative of $\left(\boldsymbol{u}_{f,i}^h, p_{f,i}^h\right)$ on the red dot is not good enough to approximate the fine scale solution on the local domain's boundary. So, it decides to enlarge the corresponding local domain to improve the approximation. In addition, we note that the red dots are almost around the end of crack where the singularity arises.

Figures 4–7 show the pressure level lines on the related adaptive meshes. It is clear that the pressure based on the VMS method is more smooth than that based on the standard Galerkin method.

In Tables I and II, we list the convergence analysis and the efficiency ratio for both the uniform and the adaptive cases. Next, we introduce some notations in both tables.

- Type 'G' means that the standard Galerkin finite element method and 'VMS' denotes the variational multiscale method.
- DOF^j (Degree Of Freedom) is the number of elements required by the numerical methods on the related iteration j.
- ς_r^j denotes the relative L^2 velocity error on the related iteration j.
- ζ_r^j means the relative H^1 velocity error on the related iteration j.
- ε_r^j denotes the relative L^2 pressure error on the related iteration j.
- e_r^j means the relative graph norm of the velocity and the pressure error on the related iteration j.

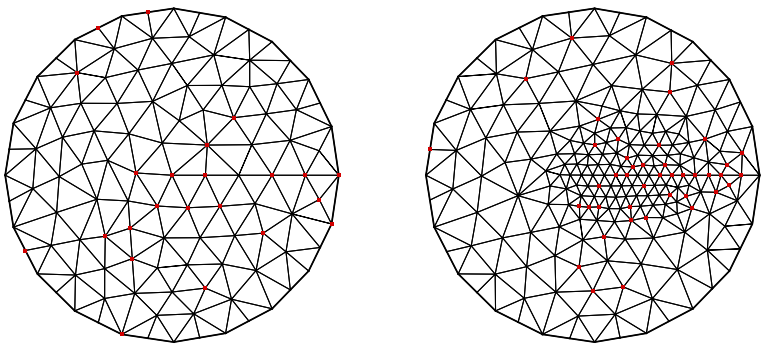

Figure 2. Left: The initial mesh τ_h^0; Right: The first adaptive mesh τ_h^1.

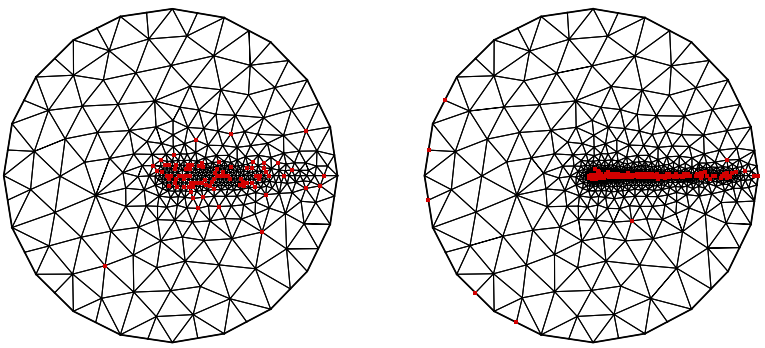

Figure 3. Left: The second adaptive mesh τ_h^2; Right: The third adaptive mesh τ_h^3.

DOI: 10.1002/fld

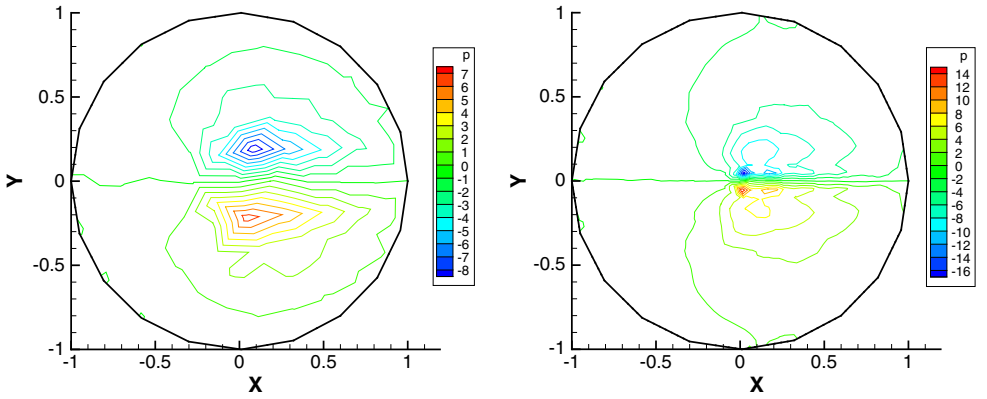

Figure 4. The pressure level line on τ_h^0 with the Galerkin method (left) and the VMS method (right).

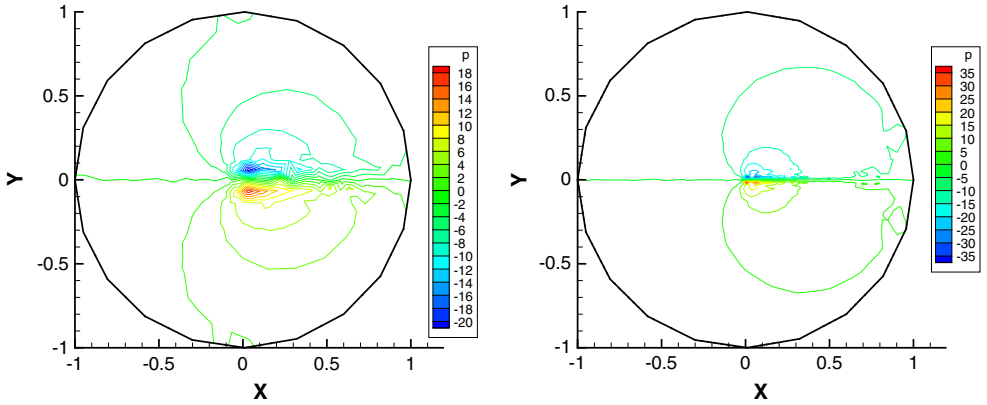

Figure 5. The pressure level line on τ_h^1 with the Galerkin method (left) and the VMS method (right).

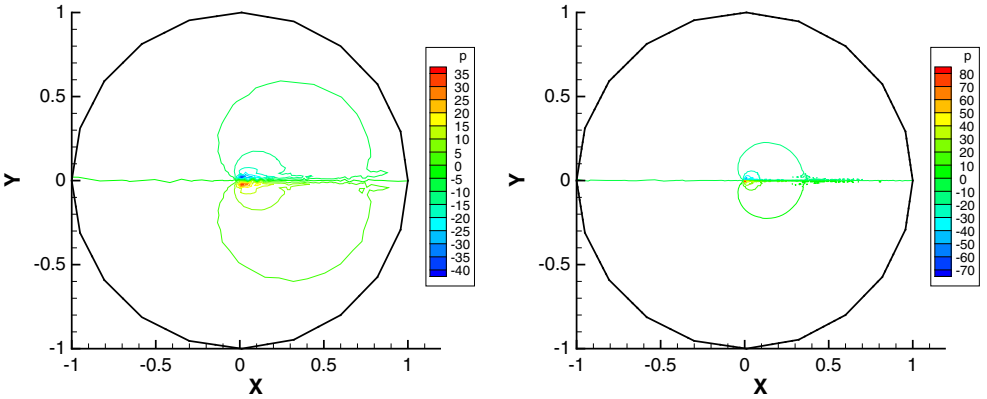

Figure 6. The pressure level line on τ_h^2 with the Galerkin method (left) and the VMS method (right).

- $E^j := \eta^j / |||\left(\boldsymbol{u} - \boldsymbol{u}_H^j, p - p_H^j\right)|||$ is the effective index, that is, the ratio between the estimated error and the standard Galerkin approximation error.
- Ratio means the experimental order of the convergence. $Ratio := \dfrac{2log\left(e_r^j / e_r^{j-1}\right)}{log\left(\frac{DOF^{j-1}}{DOF^j}\right)}$.

DOI: 10.1002/fld

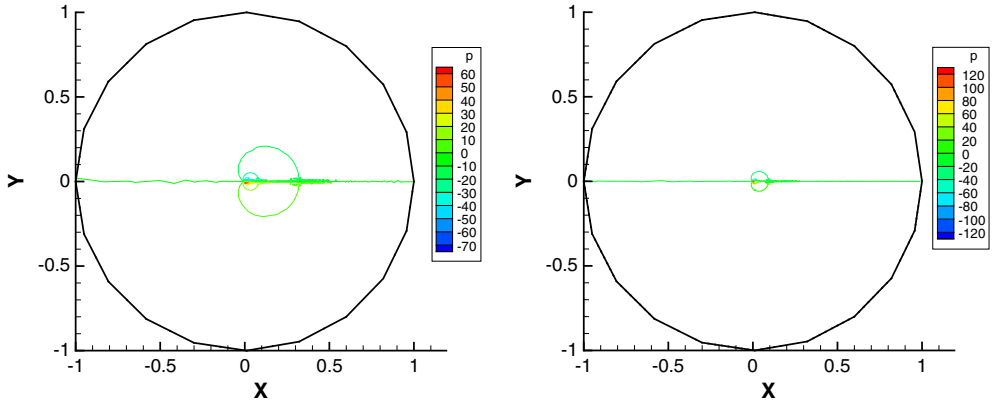

Figure 7. The pressure level line on τ_h^3 with the Galerkin method (left) and the VMS method (right).

Table I. The convergence analysis and the efficiency ratio for a sequence of adaptive meshes.

j	DOF^j	Type	ς_r^j	Ratio	ζ_r^j	Ratio	ε_r^j	Ratio	e_r^j	Ratio	E^j
0	182	G	0.07781		0.35563		0.72798		0.61214		0.35935
		VMS	0.04644	\	0.25055	\	0.48230	\	0.40898	\	
1	396	G	0.04427		0.27514		0.46455		0.40242		0.50616
		VMS	0.01487	2.92	0.15175	1.28	0.21739	2.04	0.19479	1.89	
2	866	G	0.02105		0.19263		0.26203		0.23775		0.66006
		VMS	0.00448	3.06	0.08825	1.38	0.10341	1.89	0.09786	1.75	
3	2016	G	0.00922		0.12752		0.14457		0.13826		0.81292
		VMS	0.00372	0.44	0.05081	1.31	0.05709	1.41	0.05476	1.37	

VMS, variational multiscale.

Table II. The convergence analysis and the efficiency ratio for a sequence of uniform meshes.

j	DOF^j	ς_r^j	Ratio	ζ_r^j	Ratio	ε_r^j	Ratio	e_r^j	Ratio
0	100	0.07917	\	0.35818	\	0.74005	\	0.62147	\
1	1588	0.03787	0.52	0.24771	0.26	0.39287	0.45	0.34436	0.21
2	4876	0.02585	0.68	0.20563	0.33	0.28834	0.54	0.25967	0.25
3	9980	0.01991	0.73	0.18184	0.34	0.23673	0.54	0.21727	0.24

As shown in Table I, the VMS method is much more accurate than the standard Galerkin method. Moreover, E^j increases from 0.35 to 0.8 successively. It shows the good quality of this estimator according to the definition of E^j. On the other hand, Table II shows that the uniform case does not derive a good approximation. It takes much more meshes but provides low ratios. However, the adaptive strategy obtains much better approximation with high ratios efficiently.

4.2. The Stokes flow over a step

The flow over a step is a benchmark problem which possesses the corner singularity. We consider the Stokes flow over a step with the small viscosity $\nu = 1.0e-3$. The computational domain is given by $\Omega = [0,4] \times [0,1] - [1.2,1.6] \times [0,0.4]$. The inflow at $x = 0$ is the parabolic flow $\boldsymbol{u} = (4y(1-y),0)$, whereas the outflow is the natural boundary condition. Moreover, the flow is enforced with the Dirichlet boundary condition $\boldsymbol{u} = (0,0)$ at the upper and lower boundaries. In this case, singularities arise at the step from the re-entrant corners. We expect that the adaptive strategy can refine these regions to avoid the numerical oscillation.

Figure 8 presents the successive adaptive refined meshes. The mesh refinement appears near the two corner of the step after a series of adaptive iterations. This meets the problem's requirement.

DOI: 10.1002/fld

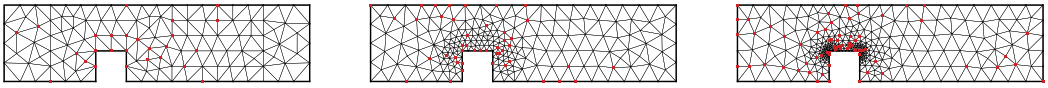

Figure 8. From left to right: The initial mesh, the first adaptive mesh, and the second adaptive mesh.

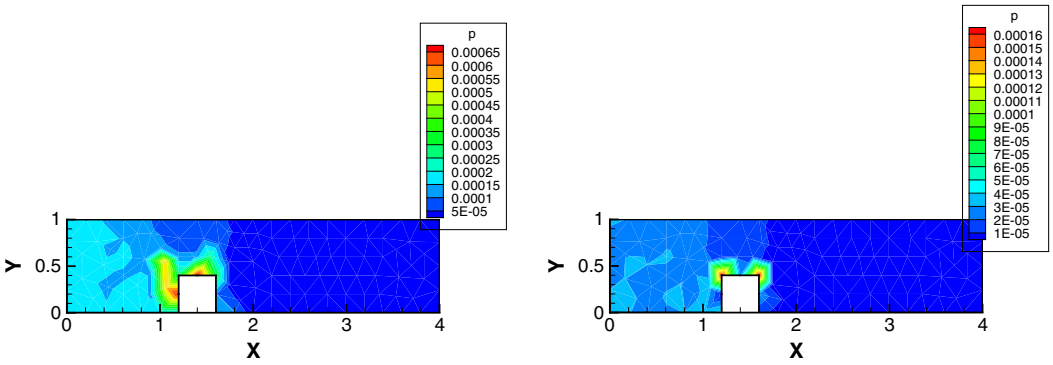

Figure 9. Error_T of the Galerkin method (left) and the VMS method (right) on τ_h^0.

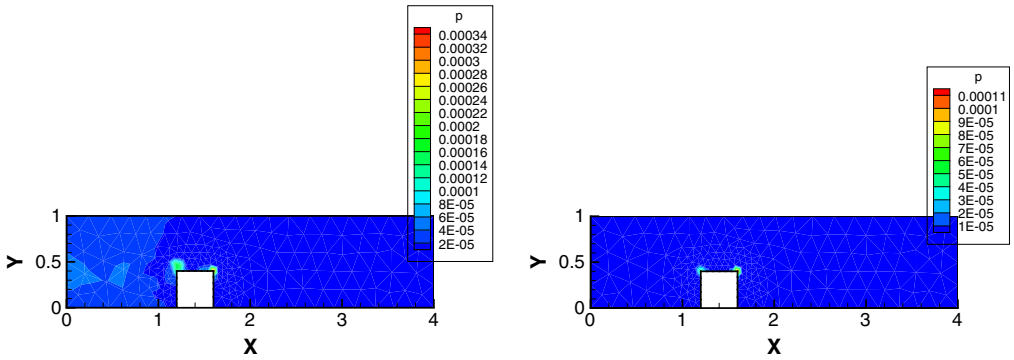

Figure 10. Error_T of the Galerkin method (left) and the VMS method (right) on τ_h^1.

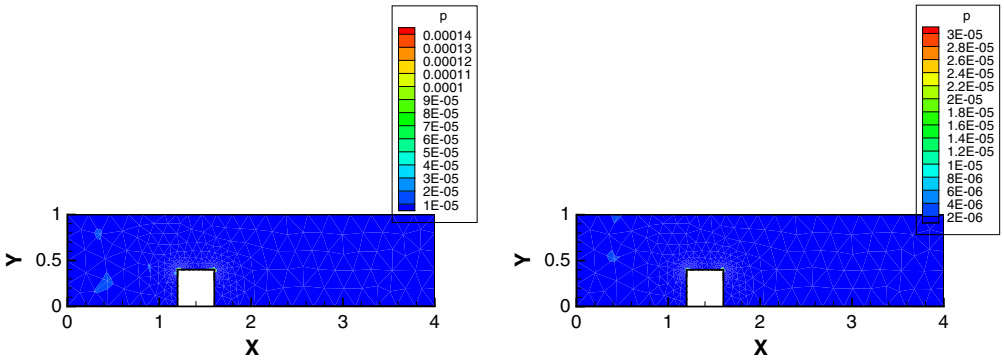

Figure 11. Error_T of the Galerkin method (left) and the VMS method (right) on τ_h^2.

Figures 9–11 show the local L^2 pressure error of both the Galerkin method and the VMS method on the relative adaptive mesh. The errors are computed by

$$\text{Error}_T = \left(\int_T (p_{hh} - p_h)^2 \mathrm{d}x \right)^{\frac{1}{2}}.$$

Here p_{hh} is obtained with the finest mesh (DOF=80,434) as the exact solution. As shown in these figures, the VMS method can obtain the more accurate approximation solution.

DOI: 10.1002/fld

4.3. The driven cavity flow

The driven cavity flow is also a standard test case in computational fluid dynamics. For the driven cavity Stokes flow, it is driven by the unit tangential velocity $\boldsymbol{u} = (1, 0)$ at the top of the unit square without the other force source. In addition, it is enforced zero on both lateral sides and the bottom side. Such discontinuity boundary conditions lead the singularities of the cavity in the two upper corners.

The left part of Figure 12 is the initial mesh. The red nodes on the mesh mean that their relevant local problems require the larger local domain. In practice, we enlarge the local domain as shown in Figure 1. The middle and left parts of Figure 12 are adaptive meshes provided by the algorithm. We can see that the mesh refinement appears in the two upper corners, which meets the problem's requirement.

Moreover, we compare the results of the adaptive VMS method with the discrete solution obtained with the much fine mesh (DOF=80000). In Figure 13, we draw $\boldsymbol{u}_1(x, y)$, the x component of the velocity, along the vertical centerline $x = 0.5$. We also draw the y component of the velocity along the horizon centerline. We can see that the results of adaptive VMS method approach the results of Galerkin method on the much fine mesh.

In Figure 14, we show the pressure level line of the driven cavity flow. It is the pressure level line of the Galerkin method on the much fine mesh in the left part. And the right part shows the pressure level line of the VMS method on the adaptive mesh. We can also see that the adaptive

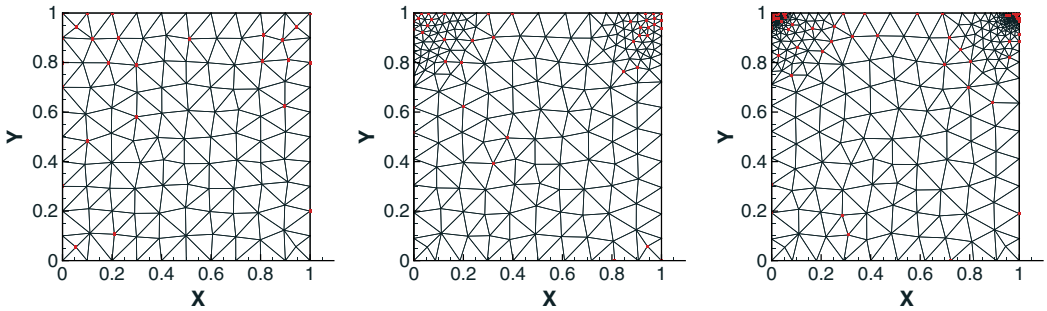

Figure 12. From left to right: The initial mesh, the first adaptive mesh, and the second adaptive mesh.

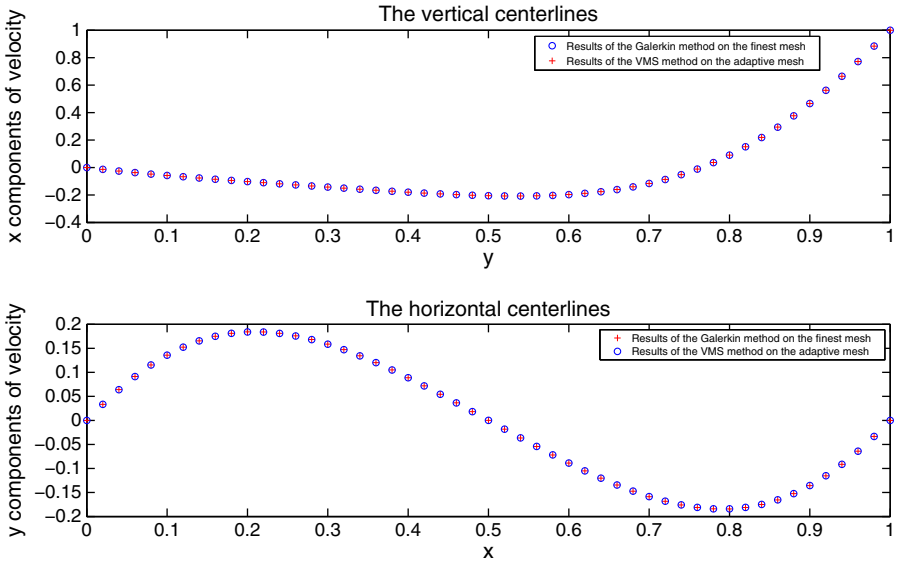

Figure 13. The centerlines for the cavity Stokes flow for Re=1.

DOI: 10.1002/fld

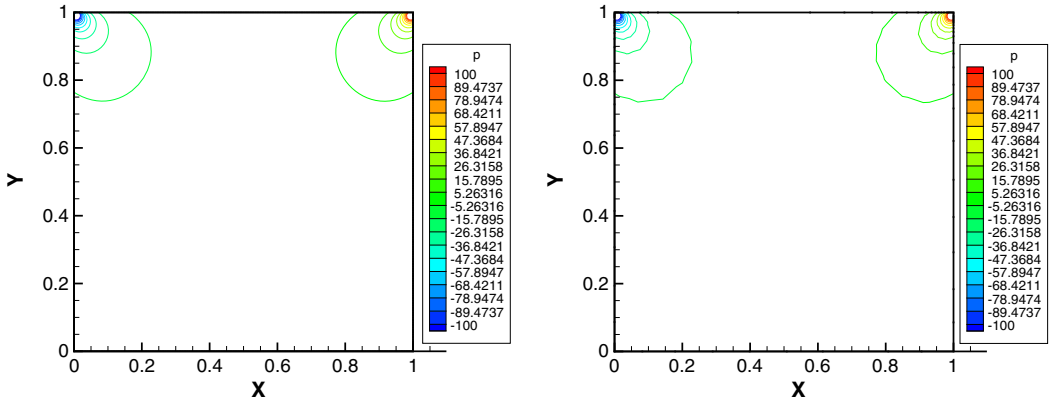

Figure 14. The pressure level lines of the Galerkin method on the much fine mesh(left) and the VMS method on the adaptive mesh (right).

VMS method uses less elements (DOF=514) to obtain the results, which are similar to that of the Galerkin method on the much fine mesh (DOF=80000). In this sense, the adaptive algorithm saves lots of memories of the computer to solve this fluid problem.

5. CONCLUSION

In this paper, we have designed and analyzed an a posteriori error estimator based on the numerical realization of the VMS method for the Stokes equations. Numerical tests showed the efficiency and reliability of the adaptive VMS method. However, there still remain some open questions, such as the parallel computation of the local problems for the fine scale equations, the correct extension of this method to the other models in fluid dynamics.

ACKNOWLEDGEMENTS

This research was supported by the NSF of China (Grant Nos. 11171269 and 11001216) and the PhD Programs Foundation of Ministry of Education of China (Grant No. 20110201110027).

REFERENCES

1. Verfurth R. A posteriori error estimators for the Stokes equations. *Numerische Mathematik* 1989; **55**:309–325.
2. Bank RE, Welfert BD. A posteriori error estimates for the Stokes problem. *SIAM Journal on Numerical Analysis* 1991; **28**:591–623.
3. Ainsworth M, Oden JT. A posteriori error estimators for the stokes and oseen equations. *SIAM Journal on Numerical Analysis* 1997; **34**:228–245.
4. Kay D, Silvester D. A posteriori error estimation for stabilized mixed approximations of the stokes equations. *SIAM Journal on Scientific Computing* 1999; **21**:1321–1336.
5. Zheng H, Hou Y, Shi F. A posteriori error estimates of stabilization of low-order mixed finite elements for incompressible flow. *SIAM Journal on Scientific Computing* 2010; **32**:1346–1360.
6. Hughes TJR. Multiscale phenomena: Green's functions, the Dirichlet-to-Neumann formulation, subgrid-scale models, bubbles and the origins of stabilized methods. *Computer Methods in Applied Mechanics and Engineering* 1995; **127**:387–401.
7. Hughes TJR, Ronzalo G, R. Feijóo L. Mazzei, J.B. Quincy. The variational multiscale method-a paradigm for computational mechanics. *Computer Methods in Applied Mechanics and Engineering* 1998; **166**:3–24.
8. Layton W. A connection between subgrid-scale eddy viscosity and mixed methods. *Applied Mathematics and Computation* 2002; **133**:147–157.
9. Kaya S, Riviere B. A twogrid stabilization method for solving the steadystate Navier–Stokes equations. *Numerical Methods for Partial Differential Equations* 2006; **3**:728–743.
10. John V, Kaya S. A finite element variational multiscale method for the Navier–Stokes equations. *SIAM Journal on Scientific Computing* 2005; **26**:1485–1503.
11. Zheng H, Hou Y, Shi F, Song L. A finite element variational multiscale method for incompressible flows based on two local Gauss integrations. *Journal of Computational Physics* 2009; **228**:5961–5971.

DOI: 10.1002/fld

12. Zheng H, Hou Y, Shi F. Adaptive variational multiscale methods for incompressible flow based on two local Gauss integrations. *Journal of Computational Physics* 2010; **229**:7030–7041.
13. Song L, Hou Y, Zheng H. A variational multiscale method based on bubble functions for convection-dominated convection-diffusion equation. *Applied Mathematics and Computation* 2010; **217**:2226–2237.
14. Larson MG, M*å*lqvist A. Adaptive variational multiscale methods based on a posteriori error estimation: energy norm estimates for elliptic problems. *Computer Methods in Applied Mechanics and Engineering* 2007; **196**:2313–2324.
15. Larson MG, M*å*lqvist A. A posteriori error estimates in the energy norm for mixed finite element methods. *Numerische Mathematik* 2008; **108**:487–500.
16. Arnold DN, Brezzi F, Fortin M. A stable finite element for the Stokes equations. *Calcolo* 1984; **21**:337–344.
17. Gunzburger M. *Finite Element Methods for Viscous Incompressible Flows: A Guide to Theory, Practice and Algorithms*. Academic Press: Boston, 1989.
18. Hughes TJR, Engel G, Mazzei L, Larson MG. The continuous Galerkin method is locally conservative. *Journal of Computational Physics* 2000; **163**:467–488.
19. Hecht F, Pironneau O, Ohtsuka K. *FreeFem++ -3.13*. 2011; (Available from: http://www.freefem.org/ff++/ftp/).

DOI: 10.1002/fld